ANNUAL REVIEWS

Annual Review of Fluid Mechanics

Fluid Dynamics of Polar Vortices on Earth, Mars, and Titan

Darryn W. Waugh

Department of Earth and Planetary Sciences, Johns Hopkins University, Baltimore, Maryland, USA; email: waugh@jhu.edu

Annu. Rev. Fluid Mech. 2023. 55:265–89

First published as a Review in Advance on October 13, 2022

The *Annual Review of Fluid Mechanics* is online at fluid.annualreviews.org

https://doi.org/10.1146/annurev-fluid-120720-032208

Keywords

vortex dynamics, atmospheric circulation, potential vorticity, Rossby waves, comparative planetology

Abstract

Polar vortices that share many similarities are found in Earth's stratosphere and the atmospheres of Mars and Saturn's moon Titan. These vortices all occur in the winter, and are characterized by high potential vorticity (PV) in polar regions, steep meridional PV gradients and peak zonal winds in middle latitudes, and a cold pole. There are, however, differences in the daily and subseasonal variability, zonal asymmetries, and PV structure among the vortices. These differences are related to differences in the disruption of polar vortices by Rossby waves, the poleward extent of the mean meridional circulation, and condensation of major gases. There are also differences in the transport of gases and particles among the vortices. The range of polar vortex characteristics is likely much larger for terrestrial exoplanets, which include planets with, for example, a wider range of obliquities.

1. INTRODUCTION

Polar vortex: a coherent structure with PV that is larger than the polar planetary PV and is centered near the pole

Potential vorticity (PV): a quantity proportional to the product of the absolute vorticity vector and gradient of potential temperature

Rossby waves: waves whose restoring force is the gradient in potential vorticity

A prominent feature of Earth's stratosphere is a band of strong westerly (west to east) winds that circumnavigate the winter pole. These so-called polar vortices play a major role in the dynamics of the stratosphere, stratosphere–troposphere interactions, and stratospheric composition. The polar vortices have been observed since the late 1940s (e.g., Scherhag 1948, Gutenberg 1949) and examined in much more detail since 1980s because of their importance for stratospheric ozone depletion (e.g., Schoeberl & Hartmann 1991). More recently, there has been a resurgence in interest in polar vortices because of their role on surface climate and weather, including the occurrence of extreme cold air events. The latter has resulted in "polar vortices" becoming a common phrase in the media, even though there is often some confusion on whether the polar vortices are in the stratosphere or troposphere (Waugh et al. 2017). Additional interest in polar vortices comes from the fact that observations over the last few decades have shown the existence of polar vortices on other planets, including Venus, Mars, Jupiter, Saturn, and Saturn's moon Titan; readers are referred to a recent review by Mitchell et al. (2021).

While the existence of polar vortices in Earth's atmosphere has been known for 70 years and they are common in the solar system, there is no universal definition of a polar vortex. The name "polar vortex" has been used to describe different atmospheric features on the same planet, including Earth (Waugh et al. 2017), Venus (Sánchez-Lavega et al. 2017), and Saturn (Fletcher et al. 2018). In addition, different fields are often used. For some planets the polar vortices are defined solely on observed polar temperature, trace gas concentrations, or cloud structures, but even when the winds can be modeled/inferred, the vortex can be defined using different meteorological fields.

From a fluid dynamical perspective, the most useful quantity for defining and understanding polar vortices is potential vorticity (PV),

$$\mathrm{PV} = \rho^{-1} \boldsymbol{\zeta}_a \cdot \nabla\theta,$$

where ρ is the fluid density, $\boldsymbol{\zeta}_a$ is the absolute vorticity vector, and $\nabla\theta$ is the gradient of the potential temperature. PV has several useful properties, including (*a*) it is materially conserved for adiabatic, frictionless flows; (*b*) other dynamical fields can be determined from its distribution (assuming an appropriate balance and given boundary conditions); and (*c*) its gradients provide the restoring mechanism for Rossby waves (e.g., Hoskins et al. 1985). This means that the PV field can be used to trace the evolution of the vortex in order to infer the impact of the changes in the vortex on the flow and to study the propagation of Rossby waves on the vortex edge.

Even if PV is the agreed-upon field, there is still no universal definition of atmospheric polar vortices. Here we use the definition proposed by Mitchell et al. (2021): "A polar vortex is a coherent structure with absolute PV that is larger than the polar planetary PV, and that is centered over or near the pole" (p. 2). Mitchell et al. (2021) further split the vortices into two types: type I, where the flow is predominantly circumpolar cyclonic flow, and type II, where the flow is of smaller horizontal scale and zonal asymmetries are large enough that a strong circumpolar flow is absent or of secondary importance. The planetary-scale polar vortices on Earth, Mars, and Titan are all type I, whereas the synoptic-scale near-tropopause polar cyclones on Earth that are referred to as "tropopause polar vortices" (e.g., Cavallo & Hakim 2009) and the recently discovered vortex clusters in Jupiter's polar regions (Adriani et al. 2018) fall into type II.

We consider here the fluid dynamics of the planetary-scale polar vortices on Earth, Mars, and Titan. Our main focus is on Earth, but by also considering the polar vortices on Mars and Titan, which are terrestrial planetary bodies with similar seasonality (obliquity; see **Table 1**), we can compare the vortex structures and dynamics and isolate the roles of different planetary parameters or processes. For example, Titan has a very different Rossby number and ratio of Rossby deformation radius to planetary radius (see **Table 1**), and Earth and Titan, but not Mars, have a

Table 1 Planetary and atmospheric parameters for Earth, Mars, and Titan

	Radius (10^3 km)	Gravity (m/s^2)	Scale height (km)	Stratosphere?	Rotation period (Earth days)	Obliquity (°)	*Ro*	L_d/a
Earth	6.37	9.8	7	Yes	1	23.5	0.1	0.3
Mars	3.40	3.7	11	No	1.03	25.0	0.1	0.6
Titan	2.58	1.4	18	Yes	16	27.0	2	10

Values are from table 1 of Showman et al. (2010).

The Rossby number $Ro = U/fL$ and Rossby radius of deformation $L_d = NH/f$ are based on the mid-latitude flow, where U is the characteristic zonal velocity, L characteristic horizontal length scale, H characteristic vertical length scale, f the Coriolis parameter, and N the Brunt–Väisälä frequency.

stratosphere. By making these comparisons, we can examine the impact of rotation rate or vertical temperature structure on the polar vortices.

Before considering the dynamics of atmospheric polar vortices, in the next section we briefly review the fundamental dynamics of regions of coherent vorticity in 2D incompressible and inviscid flows. The structure and dynamics of Earth's stratospheric polar vortices and tropospheric polar vortices are then covered in Sections 3 and 4, respectively, followed by discussion of the polar vortices on Mars (Section 4) and Titan (Section 5).

2. TWO-DIMENSIONAL VORTEX DYNAMICS

The study of 2D vortex dynamics dates back to the nineteenth century (e.g., von Helmholtz 1858, Thomson 1869, Kirchhoff 1876), and although very idealized these results are highly relevant for understanding the dynamics of polar vortices. For 2D incompressible flow, the vorticity ω can be expressed in terms of a stream function, $\omega = \nabla^2\psi$, and in the inviscid limit the vorticity is materially conserved: $d\omega/dt = 0$. The vorticity in 2D incompressible flow can therefore be thought of as the simplest case of PV: It is materially conserved and the flow can be determined from the vorticity.

The simplest vortices relevant for understanding the dynamics of polar vortices are vortices with constant vorticity ω_0 inside and zero vorticity outside, which are often called vortex patches (e.g., see chapter 9 of Saffman 1992). A circular vortex patch (Rankine vortex) rotates with constant angular velocity ($\Omega = \omega_0/2$) and is linearly stable, and perturbations to the edge of the vortex propagate against the mean flow with constant angular velocity $\omega_0/2m$ (where m is the azimuthal wavenumber) (e.g., Lamb 1945, Saffman 1992). The restoring mechanism responsible for this wave propagation is provided by the presence of the vorticity gradient at the vortex edge, and these waves can be considered as interfacial Rossby waves. The propagation against the mean flow is in fact the characteristic signature of westward-propagating Rossby waves.

An elliptic patch of vorticity (Kirchoff vortex) also maintains its shape and simply rotates about its center at a steady rate in the absence of background flow (Kirchhoff 1876, Saffman 1992). Furthermore, a Kirchoff vortex is linearly stable if it is not too elongated, specifically if its aspect ratio is less than 3 (Love 1893). Numerical calculations show that the instability for elongated vortices generally results in the production of long, thin filaments of vorticity (e.g., Dritschel 1986, Polvani et al. 1989). The Kirchoff vortex remains elliptical under the application of some combination of uniform advection, rotation, and strain (Moore & Saffman 1971, Kida 1981). Specifically, Kida (1981) showed that the patch remains elliptical in a time-varying surrounding flow with uniform strain and rotation but that the orientation and aspect ratio generally vary with time, with a rich phenomenology including periodic (rotating or nutating) solutions or extending/compressing solutions. Dritschel (1990) further showed that there is a very complex instability structure for these vortices, with instability and generation of filaments occurring for much of the parameter space explored.

The generation of long, narrow filamentary structures found in nonlinear simulations of unstable patches is a ubiquitous feature of simulations of multiple vortices (e.g., Dritschel 1995) and 2D turbulence (e.g., Bracco et al. 2000, Boffetta & Ecke 2012). This filamentation can be viewed as a simple kinematic mechanism associated with the existence of a stagnation point in the corotating flow coinciding with the vortex contour (e.g., Polvani et al. 1989). Another pathway is the nonlinear steepening of waves (Dritschel 1988).

The ubiquitous nature of filaments is somewhat surprising, as infinite strips or annuli of constant vorticity are unstable (Rayleigh 1880, Dritschel 1989) and break up into a series of small-scale vortices. This instability occurs when waves on either side of the region of constant vorticity interact with each other and hold themselves stationary against the background flow. This phase-locking is analogous to that occurring for Rossby waves in baroclinic instability (e.g., Hoskins et al. 1985). However, this phase-locking can be suppressed by a background straining flow (Dritschel 1989, Dritschel et al. 1991), and the robustness of filaments surrounding vortices is likely due to the stabilizing effect of the straining flow generated by the vortex.

The studies reviewed above have considered the very idealized case on a single region of uniform vorticity, which may seem too unrealistic for application to atmospheric polar vortices (or vortices in the atmosphere and oceanic flows more generally). However, simulations of the vortices with distributed vorticity in strain/shear flows show that filamentation erodes the exterior layers of the vortex and generates very high vorticity gradients at the edge of the vortex (e.g., Legras et al. 2001). This phenomenon, called vortex stripping, leads to vortices with relatively uniform vorticity and a very sharp edge, and it is ubiquitous in simulations of interacting vortices (including in simulations of 2D turbulence). Thus, consideration of the dynamics of vortex patches is more appropriate than may be first thought.

The above discussion has focused on planar barotropic flow, but most of the results carry over to barotropic spherical flows (e.g., Polvani & Dritschel 1993), shallow-water flows (e.g., Waugh & Dritschel 1991, Płotka & Dritschel 2012), and 3D flows (e.g., Reinaud & Dritschel 2019). Furthermore, the key results of the stability of near-circular vortices, the generation of stable filaments, and vortex stripping and the formation of steep PV gradients are common features in the atmospheres and oceans, including, as discussed below, planetary polar vortices.

3. EARTH'S STRATOSPHERIC POLAR VORTICES

Earth has two distinct planetary-scale features that have been called polar vortices, one that is in the stratosphere (1–100 hPa; 15–50 km) and the other in the upper troposphere. We discuss the stratospheric polar vortex here and consider the (somewhat controversial) tropospheric polar vortex in Section 4.

3.1. Climatological Structure

Earth's stratospheric polar vortices exist during fall to spring when the polar region is in darkness and the lack of solar heating leads to low polar temperatures and large-scale temperature gradients across mid-latitudes. Accompanying these meridional temperature gradients are strong westerly winds in mid-latitudes, which are in approximate thermal wind balance [$\partial u/\partial p = (R/fp)(\partial T/\partial y)$; e.g., chapter 2 of Vallis (2017)] (**Figure 1**), and a coherent region of large PV centered on or near the pole (**Figure 2**). Note that PV is negative in the Southern Hemisphere (SH), and when we refer to large PV we are referring to large absolute values in the SH. The polar vortices strengthen from fall into winter, break down as sunlight returns to the polar regions in spring, and then the winds become weak easterlies in the summer (**Figure 1**).

While the Arctic and Antarctic polar vortices have qualitatively similar structure and evolution, there are important quantitative differences. The Antarctic vortex is broader, stronger (in terms

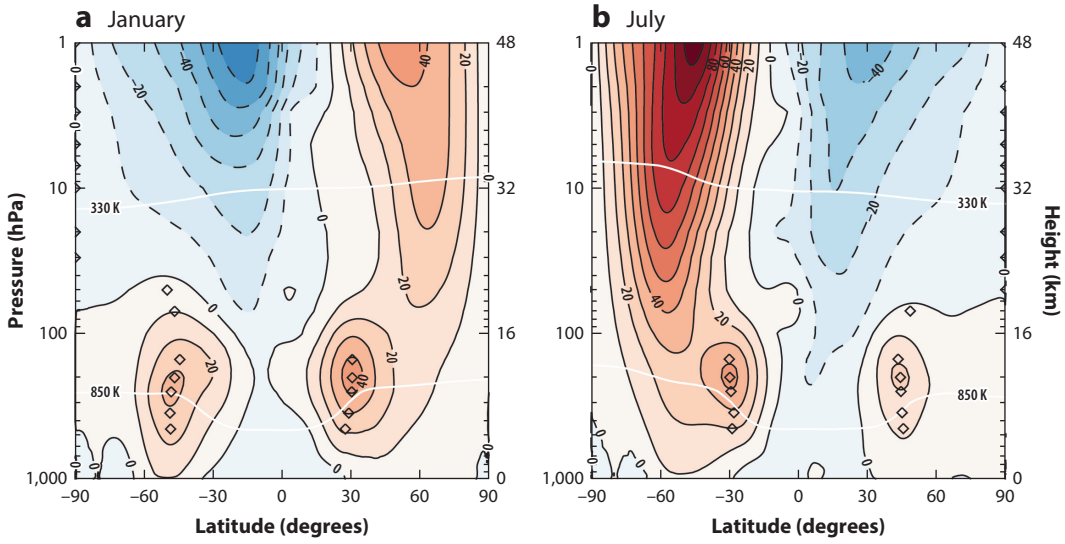

Figure 1

Climatological longitudinally averaged (zonal-mean) zonal wind in (*a*) January and (*b*) July. Contours demarcate every 10 m/s, with red colors for positive (westerly) winds and blue for negative (easterly) winds. Left *y*-axes show pressure (hPa) and right *y*-axes show height above the ground (km). The diamonds mark the hemispheric maximum of the zonal wind at each pressure level and the approximate edge of the polar vortex for that hemisphere. White contours show the 330 K and 850 K isentropic surfaces. Data from the European Centre for Medium-Range Weather Forecast's ERA5 reanalysis (Hersbach et al. 2019), accessed May 2022.

of PV and winds), and more zonally symmetric (**Figure 2**), and it has less temporal variability and a longer lifespan (e.g., Waugh et al. 1999). Additionally, the minimum polar temperatures in the Antarctic are lower and stay colder for longer than they do in the Arctic (see, e.g., figure 3 of Lawrence et al. 2018). These differences in polar temperatures are the cause of hemispheric differences in polar ozone depletion: In the Antarctic, the temperatures are low enough for the formation of polar stratospheric clouds (PSCs) and chemical destruction of ozone every year, but in the Arctic temperatures fall below this threshold much less frequently and there is more limited ozone destruction (with large variations between years) (Solomon 1999).

3.2. Polar Vortex and Rossby Wave Dynamics

The above hemispheric differences in the polar vortex are caused by differences in the generation of Rossby waves between hemispheres. Rossby waves generated in the troposphere propagate up into the stratosphere (e.g., chapter 16 of Vallis 2017) and perturb the vortices away from radiative equilibrium (the equilibrium when solar heating balances infrared cooling). This weakens the vortices, makes them less zonally symmetric, and causes temporal variability. There are larger topography and more land–sea contrasts in the Northern Hemisphere (NH) that push the Arctic polar vortex further from radiative equilibrium than there is in the SH. These differences in wave generation explain not only the climatological structure of the vortices but also their temporal variability, since much of the variability in the polar vortices is linked to changes in the upward wave propagation.

Maps of PV provide critical insights into the dynamics of the polar vortices. **Figure 3** shows PV maps for several days during January and February 1979. This figure shows that there can be large variability in the structure of the polar vortex, with periods when the vortex is near-circular and centered on the pole, and others when the vortex is distorted and displaced from the pole.

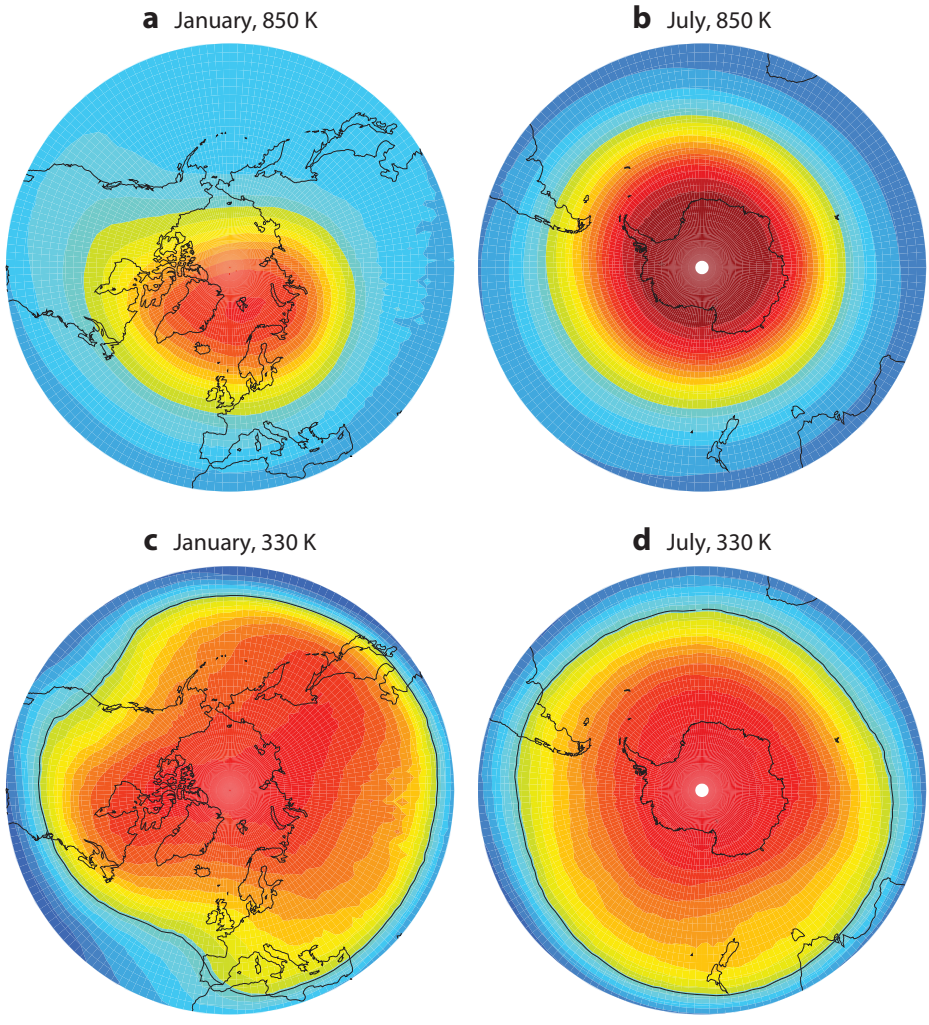

Figure 2

Maps of the climatological mean potential vorticity (PV) winds on isentropic surfaces for (*a*) Northern Hemisphere (NH), January, at 850 K; (*b*) Southern Hemisphere (SH), July, at 850 K; (*c*) NH, January, at 330 K; and (*d*) SH, July, at 330 K. Black contours in panels *c* and *d* show the absolute PV = 3×10^{-6} K m^2 kg^{-1} s^{-1}. Data from the European Centre for Medium-Range Weather Forecast's ERA5 reanalysis (Hersbach et al. 2019), accessed May 2022.

Sudden stratospheric warming (SSW): a large, rapid increase in polar temperatures in the stratosphere

The latter includes a period (late January) when the vortex is elongated with a filament of high PV extending into mid-latitudes (with filaments of low PV from the subtropics extending to high latitudes), and another (late February) when the vortex splits into two smaller regions of high PV. There is an increase in polar temperature in the periods when the vortices are distorted, and these are termed "sudden stratospheric warming" events (SSWs), as discussed further below.

The period shown in **Figure 3** was considered in the seminal study of McIntyre & Palmer (1983) (see also McIntyre & Palmer 1984). They examined maps of PV from objective analyses of available radiosonde and satellite data, which had a much lower resolution than the modern reanalyses and provided only a coarse-grained view of the PV field. In particular, the old analyses

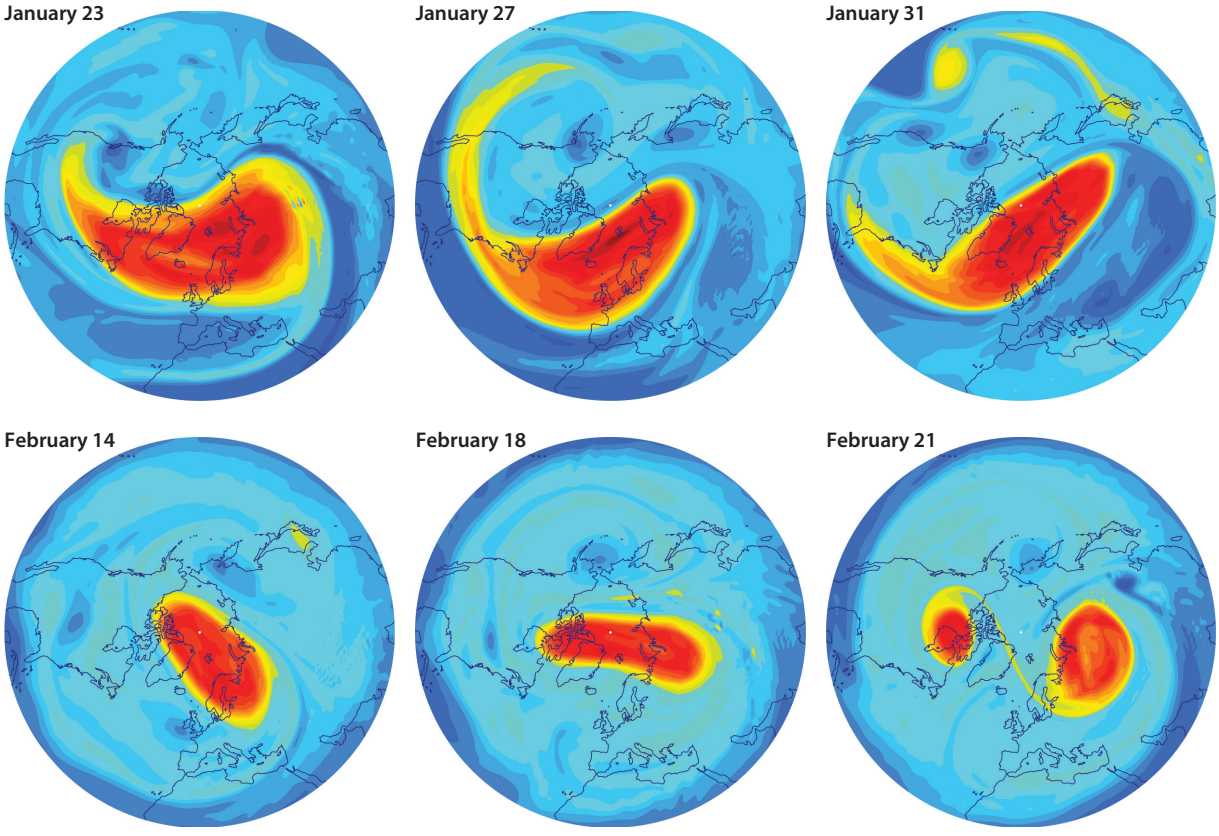

Figure 3

Maps of potential vorticity on the 850-K isentropic surfaces for several days during January and February 1979, from ERA-Interim reanalyses. Maps are polar stereographic projections with an outer edge at 20° N. Data courtesy of Will Seviour.

showed blobs rather than filaments and relatively weak gradients at the edge of the vortex. However, building off of classical vortex dynamics (Section 2), McIntyre & Palmer associated reversible distortions of the vortex with propagating Rossby waves, and contrasted these with irreversible deformations where air with high PV is pulled off of the vortex and stirred into mid-latitudes (e.g., late January 1979). Using an analogy with ocean surface waves, they referred to the latter process as Rossby "wave-breaking," and to the region surrounding the vortex as the "surf zone."

The propagation of waves around the polar vortex, the generation of filaments that wrap around the vortex, vortex erosion and gradient intensification, and the vortex splitting shown in **Figure 3** are all features found for vortices in 2D incompressible and inviscid flows (Section 2). These features are also found in a hierarchy of polar vortex simulations, including idealized models where the vortex is represented by a single region of uniform PV (Polvani & Plumb 1992) (**Figure 4*a***), single-layer spherical models (e.g., Juckes & McIntyre 1987, Norton 1994, Polvani et al. 1995) (**Figure 4*b***), and 3D models (see Haynes 1990, Dritschel & Saravanan 1994, Waugh & Dritschel 1999, Polvani & Saravanan 2000) (**Figure 4*c***). In all cases illustrated in **Figure 4**, an initially zonally symmetric vortex is disturbed by topographic-forcing (to mimic the impact of upward-propagating Rossby waves), exhibiting Rossby wave-breaking, stirring of filaments into middle latitudes, and (in cases with continuous PV distributions) vortex erosion. For 3D flows

Rossby wave-breaking: the rapid amplification and irreversible deformation of potential vorticity contours

Surf zone: the area surrounding the polar vortex where breaking Rossby waves stir potential vorticity, resulting in weak meridional gradients

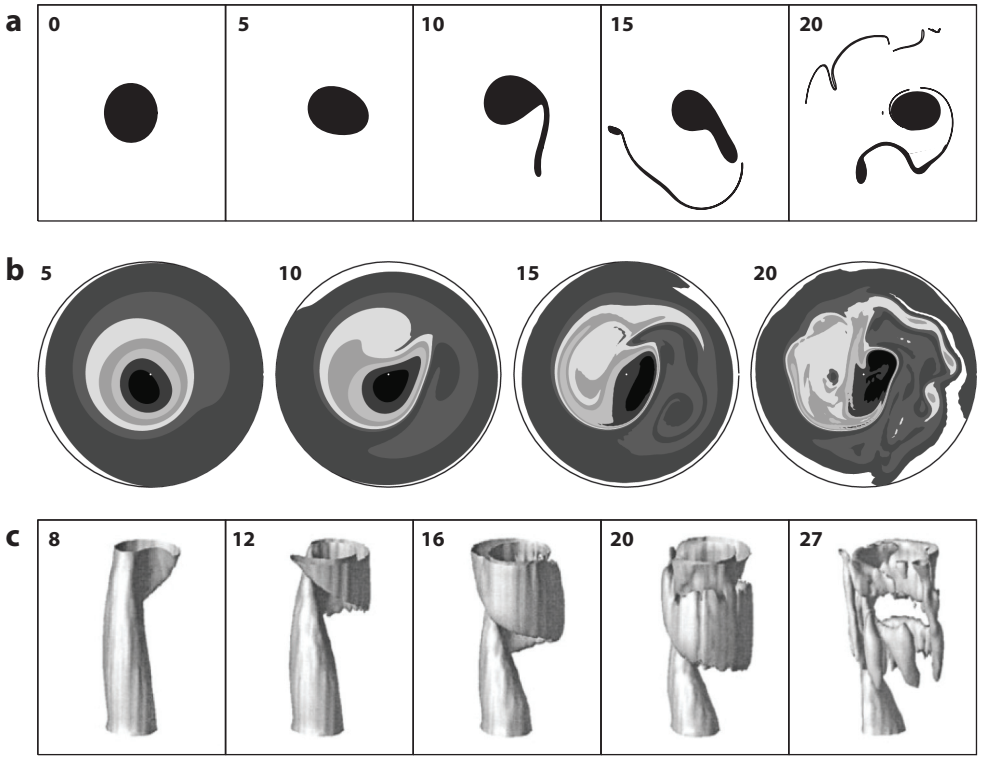

Figure 4

Simulations of polar vortices disturbed by stationary topographic-forcing with zonal wavenumber 1 for a hierarchy of models: (*a*) a planar, quasi-geostrophic model with a vortex represented by a single discontinuity in potential vorticity (PV) (Polvani & Plumb 1992); (*b*) a spherical shallow-water model with a continuous PV distribution (e.g., Polvani et al. 1995); and (*c*) a 3D spherical primitive equation model (Polvani & Saravanan 2000). Numbers indicate the elapsed time, in days, since the start of the simulations. Figure adapted from Waugh & Polvani (2010); copyright 2010 American Geophysical Union.

the wave-breaking can occur at different levels, including cases where this breaking occurs only at upper levels (**Figure 4*c***), as well as cases where wave-breaking at lower levels can inhibit further wave propagation (and breaking) into the upper levels.

The wave-breaking and vortex erosion shown in **Figures 3** and **4** will, in the case of large topographic-forcing, lead to destruction of the vortex if there is no restoring process. In reality this restoring process is radiation, which during winter leads to a cooling of the pole relative to mid-latitudes. In idealized models this is often parameterized as relaxation back to an equilibrium height [for shallow-water models (SWMs)] or temperature (for 3D models), and inclusion of this relaxation can lead to a persistent vortex whose structure is determined by the balance between erosion by wave-breaking and relaxation back to the defined equilibrium.

3.3. Extreme Events

As discussed above, there can be large daily variability in the polar vortex structure and strength, especially in the NH. This includes periods of very strong (near zonally symmetric) vortices, as well as periods with weak (highly distorted) vortices. These extreme events have been linked to anomalous time-integrated (~40 day) wave activity preceding the events, with strong (weak) wave

activity preceding weak (strong) vortex events (e.g., Christiansen 2001, Polvani & Waugh 2004). As shown by Newman et al. (2001) (see also Esler & Scott 2005), stratospheric polar temperatures on a given day are related not to the instantaneous upward wave activity but to its weighted integral over several weeks prior to that day.

While this strong connection between time-integrated wave-forcing and vortex strength suggests that polar vortex variability is determined by tropospheric wave-forcing, it is important to remember that the troposphere and stratosphere are coupled and the variability of waves propagating into the stratosphere is likely influenced by the stratospheric conditions. This can be seen in idealized model simulations with constant topographic-forcing. When forcing is large, vacillations can occur where the flow cycles between a stage when there is no vortex (or a smaller remanent vortex) and a stage with a strong vortex (e.g., Holton & Mass 1976, Scott & Haynes 2000, Rong & Waugh 2004, Scott & Polvani 2004). These vacillations can be related to the dependence of Rossby wave propagation on the existence of PV gradients: When there is a strong vortex with steep gradients there is wave propagation and wave-breaking that lead to the breakdown of the vortex, which results in weak PV gradients and limited wave propagation and breaking, and the vortex rebuilds (by relaxation) until PV gradients develop such that wave propagation and wave-breaking occur. Thus, fluctuations between strong and weak vortices can occur even if there is no change in forcing.

Strong vortex events correspond to periods with very low polar temperatures. As discussed above, very low temperatures lead to the formation of PSCs and ozone depletion. Thus, in winters when there are persistent, strong Arctic vortices there can be substantial Arctic ozone loss. An example of this was the recent 2019–2020 northern winter, which had a very strong polar vortex and the lowest ever total column ozone observed in the February–April period (see the American Geophysical Union's 2022 special collection titled The Exceptional Arctic Stratospheric Polar Vortex in 2019/2020: Causes and Consequences; **https://doi.org/10.1029/2022JD037381**).

Conversely, weak vortex events correspond to periods with a warmer pole, and to no or very limited ozone depletion. During these events there are large, rapid temperature increases in the winter polar stratosphere, and they generally correspond to SSWs. If there is also a reversal of the direction of the zonal-mean zonal winds during the event then they are called major SSWs. There is a long history in studying SSWs (with first observations in 1952) and an extensive literature: Readers are referred to Baldwin et al. (2021) for a recent review, Butler et al. (2015) for a discussion of the definitions of SSWs, and Butler et al. (2017) for a compendium of SSW events.

Major SSWs occur on average around once every two years in the NH (Butler et al. 2017) and have traditionally been classified as zonal wavenumber 1 (wave-1) or wavenumber 2 (wave-2) events depending on the amplitude of the zonal wavenumber around 60° N. However, there has been a more recent movement toward classifying the events as either a vortex displacement or a vortex split. The January and February 1979 events shown in **Figure 3** are examples of vortex displacement and vortex split events, respectively. The vertical structure has been shown to differ between events (splitting events are barotropic, while the vortex tilts westward with height for displacements), and there are also differences in the influence on the troposphere (e.g., Seviour et al. 2016).

While there has been extensive analysis of SSWs, there remain large uncertainties in the dynamics involved. Baldwin et al. (2021) divided dynamical theories for SSWs into bottom-up and top-down perspectives. Historically, analysis of the dynamics of SSWs, starting with seminal studies by Matsuno (1970, 1971), has focused on the bottom-up perspective, with the SSW being caused by strong planetary wave-forcing from the troposphere (e.g., Andrews et al. 1987). The SSWs have been linked to exceptional pulses of wave activity, either because of tropospheric

precursor events or because the stratospheric vortex was preconditioned so to speak (McIntyre 1982). An alternate perspective is the top-down view, where fluctuations in the tropospheric wave-forcing are not needed and the SSW occurs because of processes within the stratosphere (assuming sufficiently strong wave-forcing). This perspective has focused primarily on the resonant excitation of free modes (e.g., Tung & Lindzen 1979, Plumb 1981, Esler et al. 2006, Matthewman & Esler 2011). A third perspective focuses on vortex–vortex interactions rather than upward wave propagation, either between the polar vortex and Aleutian anticyclone (e.g., O'Neill & Pope 1988, Scott & Dritschel 2006) or between the polar vortex and synoptic scale tropospheric vortices (O'Neill et al. 2017). There is evidence for all proposed mechanisms, and the cause (or causes) of SSWs remains unclear.

Hadley cell: a large-scale meridional circulation cell, with ascending air in the summer hemisphere and descending air in the winter hemisphere

The probability distribution function of the vortex strength is close to Gaussian, consistent with a random process (Baldwin & Dunkerton 2001, Polvani & Waugh 2004). However, there is evidence for a decreasing frequency of strong vortex events and an increase in events since 1979 (e.g., Kretschmer et al. 2018). There is also evidence for a shift in the center of the vortex of this period (Zhang et al. 2016). It is, however, unclear how much of these changes are a forced response (e.g., responses to climate change) as opposed to natural internal variability (Seviour 2017). The future trends in SSWs in the NH are also very uncertain, with some models showing an increase in SSW while others showing a decrease (Ayarzagüena et al. 2020).

The above discussion of strong and weak vortices has focused on the Arctic vortex, as it is much more variable and SSWs are much more common there. However, a major SSW did occur in the SH in September 2002. This is the only southern SSW in the six decades of station data (e.g., Charlton & Polvani 2007). Another SSW occurred in 2019, but it was not accompanied by a wind reversal at 10 hPa and, hence, was not classified as a major SSW. Both the 2002 and 2019 SSWs resulted in very small ozone holes (Safieddine et al. 2020), and the 2019 event has been linked to the bushfires in Australia (Lim et al. 2021). The fact that no SSWs were observed in the SH before 2002 and that another SSW occurred in 2019 raises the possibility that climate change is causing the frequency of SSWs to change. However, analysis of long simulations with constant greenhouse gases indicates that SSWs in the SH should occur around once every 22 to 25 years (Wang et al. 2020, Jucker et al. 2021), and the observational record is consistent with the random occurrence of rare events. Furthermore, simulations with increased CO_2 indicate that the frequency of SH SSWs, as well as minor vortex-weakening events, will decrease rather than increase with CO_2 and that by the end of this century southern SSWs will be even rarer (Jucker et al. 2021).

3.4. Connections to Tropospheric Climate and Weather

The base of the stratospheric polar vortices is around 16 km (100 hPa), with weaker coherence of polar PV and weaker winds below this level [in a region sometimes called the subvortex (McIntyre 1995)]. This base is well above the mid- and high-latitude tropopause, but the stratospheric vortices can still influence tropospheric climate and weather. This influence applies for daily, seasonal, and interannual timescales and has received a lot of attention in recent decades [see recent reviews by Domeisen & Butler (2020) and Scaife et al. (2022)].

At decadal timescales, examples of the tropospheric influence are seen in trends in the summer tropospheric circulation in the SH during the 1980s and 1990s. During this period there was a strengthening, and a delay in the breakup, of the Antarctic polar vortex due to the ozone hole–induced polar cooling, and this has been connected to a wide range of changes in the tropospheric, and even ocean, circulation (e.g., Thompson et al. 2011). This includes a poleward shift of the tropospheric eddy-driven jet and edge of the Hadley cell [although internal atmospheric variability likely also played a role in these shifts (Garfinkel et al. 2015)]. Since 2000 there have been a

stabilization of the ozone hole and, associated with this, pauses in the polar vortex strengthening and the poleward shift in the tropospheric flow (Banerjee et al. 2020).

In the NH, there is a well-documented connection between weak and strong Arctic stratospheric vortex events and surface weather (Baldwin & Dunkerton 2001). Specifically, anomalous surface weather in northern mid-high latitudes can persist for up to 60 days following weak or strong vortex events. Furthermore, a range of surface extremes have been linked to extreme polar vortex events. For example, it has been shown that the probability of so-called cold air outbreaks (advection of an extremely cold air mass from the polar regions to the middle-lower latitudes at the surface) increases following periods when the stratospheric vortex is highly disturbed and weakened (Thompson et al. 2002, Kolstad et al. 2010). Other surface impacts linked to the polar vortex include sea ice extent, storm tracks, and droughts (see Domeisen & Butler 2020 and references therein).

While strong connections have been shown to exist between the stratospheric polar vortex and the tropospheric climate and weather, there remains much uncertainty in the exact mechanism involved. Several mechanisms by which changes in the stratospheric vortices could influence the troposphere have been proposed, including remote effects of wave-driving in the stratosphere (so-called downward control), changes in the reflection and absorption of planetary waves, the remote impact of PV anomalies, or changes in phase speed and length scales of baroclinic eddies (for a summary, see Baldwin et al. 2021). In addition to these mechanisms for the initial tropospheric response, there are subsequent changes due to eddy–mean flow interactions within the troposphere. There is some indication that the impact on the tropospheric changes from these tropospheric feedbacks is much larger than the initial stratospheric impact from the abovementioned mechanisms (Garfinkel et al. 2013).

3.5. Tracer Transport

Low temperatures, and, hence, the formation of PSCs and the chemical destruction of ozone, within the polar vortices are not the only way the vortices influence the stratospheric distribution of ozone and other trace gases. The quasi-horizontal exchange of air across the edge of the polar vortices also plays a key role. The transport of (non-ozone-depleted) air from mid-latitudes in the vortex can offset some of the depletion within the vortex, while transport of ozone-depleted air out of the vortex can lead to ozone depletion in mid-latitudes.

High-resolution simulations of tracers show structures very similar to PVs (as expected given that PV is also a tracer over short timescales): Wave-breaking at the edge of the vortex strips filaments of tracer from the vortex edge and stirs them into the mid-latitude surface (a similar stirring in of tracer filaments occurs from the subtropics) (e.g., Waugh et al. 1994). Stirring and mixing homogenize tracers with the surf zone, with very steep gradients at the vortex edge and, to a lesser degree, in the subtropics. Consistent with this, estimates of effective diffusivity show large values equatorward of the vortex edge (jet) and very low values at the vortex edge (Haynes & Shuckburgh 2000, Allen & Nakamura 2001, Abalos et al. 2016). These tracer filaments and steep gradients at the vortex edge found in these simulations have been verified by aircraft observations (e.g., Waugh et al. 1994, Plumb et al. 1994).

While the transport is generally from the vortex edge into mid-latitudes, there are events where the vortex is highly distorted, and the wave-breaking mixes surf zone air into the vortex. This is seen in both simulations and observations (Plumb et al. 1994). Hence, the vortex edge is not a complete barrier to inward transport. In the so-called subvortex (below 16 km), there is increased mixing between polar and mid-latitudes, and tracers are stirred between the polar lowermost stratosphere and the subtropical tropopause.

4. EARTH'S TROPOSPHERIC POLAR VORTICES

The term "polar vortex" is not used exclusively to describe the stratospheric feature discussed in the previous section. The term "tropospheric circumpolar vortex" has been used in the scientific literature since the 1940s to describe the hemispheric-scale flow in the upper troposphere, and this has been abbreviated to "tropospheric polar vortex" over time (see Waugh et al. 2017 and references therein). Historically tropospheric polar vortex studies have defined the vortex using specified contours of geopotential height on pressure levels of 300 or 500 hPa that lie within the core of the upper tropospheric westerlies (i.e., the vortex edge generally lies between 40° and 50° N; see **Figure 1**). As with the stratospheric vortex, the upper tropospheric jet occurs where there are strong meridional temperature gradients and is largely in thermal wind balance. However, in contrast to the stratosphere, the jet is at the descending branch of the Hadley cell and is influenced by baroclinic instability.

From a PV perspective, the edge of the tropospheric vortex can (as in the stratosphere) be defined from PV contours on an isentropic surface. The 300–500 hPa geopotential height contours that have historically been used to define the vortex are similar to the intersection of the PV = 3×10^{-6} K m^2 kg^{-1} s^{-1} surface with the 330-K isentropic surfaces (**Figure 2**) (i.e., the tropospheric polar vortex edge could be defined as where the mid-latitude tropopause crosses the 330-K isentropic surfaces). Using such a definition, one can show the tropospheric polar vortex to have many of the features described above for stratospheric polar vortices (and 2D vortex dynamics): steep PV gradients at the vortex edge, propagation and breaking of Rossby waves along these gradients, the generation of filaments on high PV that are stirred into the low-PV troposphere, and vortex stripping and gradient intensification (e.g., Holton et al. 1995, Appenzeller et al. 1996). Furthermore, as discussed in detail by Hoskins et al. (1985), synoptic weather events, such as cut-off lows, blocking events, and extreme cold events, can be understood in terms of PV dynamics along the dynamical tropopause (or, equivalently, along the edge of above-defined tropospheric polar vortex).

The term "tropospheric polar vortex" has a much more limited use in the scientific literature than that of "stratospheric polar vortex." However, following the extreme cold air outbreak over the United States in 2014, polar vortices have received a lot of attention in the mainstream media and popular science websites, which has resulted in increased usage in the scientific literature (see Manney et al. 2022). There is some debate concerning whether consideration of a tropospheric polar vortex adds significant new insights to the traditional descriptions in terms of ridges and troughs, or in terms of waves propagating along the upper tropospheric jet stream (Waugh et al. 2017, Manney et al. 2022). Manney et al. (2022) suggested that salient features of the tropospheric circulation can most clearly be described in relation to the tropospheric jet streams, without invoking the term "tropospheric polar vortex." This is likely true, and there is currently limited evidence for added value from consideration of a tropospheric polar vortex. However, there have been few studies examining the dynamics of this so-called polar vortex, and it may still be worth considering its usage.

Consideration of a tropospheric polar vortex (as opposed to, for example, separate jet streams) may enable vortex dynamics theory and concepts to be applied to understand the tropospheric flow. It also opens the possibility of examining stratosphere–troposphere dynamical interactions from a vortex–vortex perspective. In the most idealized sense, the system could be viewed as a small, vertically extended vortex (the stratospheric vortex) with a larger, more vertically confined vortex below (the tropospheric vortex). Whether this perspective will provide new insights is unknown. A different reason for considering a tropospheric polar vortex is for comparisons with the Martian polar vortices, as discussed in the next section.

5. MARS

The polar vortices that exist in Mars's atmosphere share many characteristics with Earth's stratospheric vortices: In both cases the vortices form in the fall and decay in the spring, have strongest westerly winds (jet) at mid-to-high latitudes, high PV poleward of the jet, and low temperatures over the pole (e.g., Mitchell et al. 2015; Waugh et al. 2016) (see **Figure 5**). There are, however, several differences between the Martian and Earth polar vortices: The NH winter vortex is stronger than its SH winter counterpart on Mars, the areal extent of the vortex decreases with altitude on Mars (**Figure 5**), and Martian polar vortices exhibit less temporal variability. More significantly, there are differences in (*a*) the formation mechanism and (*b*) the PV structure.

Considering the formation mechanism first, although there are the above similarities with Earth's stratospheric vortex, the polar vortex on Mars is in the troposphere (there is no stratosphere on Mars) and actually exhibits more similarities in the formation with Earth's tropospheric polar vortices. Both the Martian and Earth's tropospheric polar vortices are directly connected to the tropospheric Hadley cell, with the vortex edge (westerly jet) forming at the descending branch of the Hadley cell. In addition, for both vortices, the PV on the equator side of the jet is close to zero, consistent with an angular momentum conserving flow within the Hadley cell (Waugh et al. 2016, Scott et al. 2020).

The size of the polar vortices (latitude of jets) differs between Martian and Earth tropospheric polar vortices, but this is again directly tied to the Hadley cells. On Mars the solstitial Hadley cell is much broader than it is on Earth, with a single cell that ascends in summer high latitudes and descends at winter high latitudes (compared to an ascending branch near the equator and a descending branch around 30° on Earth). This results in the strongest westerlies (and edge of the polar vortex) being at much higher latitudes on Mars than in Earth's troposphere. The hemisphere difference in Mars's polar vortices is also connected to the Hadley cells: The northern winter single Hadley cell is broader and stronger during southern winter [due primarily to the difference in topography between hemispheres (Richardson & Wilson 2002, Zalucha et al. 2010)], which results in a northern winter vortex that is smaller than its southern counterpart.

While the formation mechanism is the same for Mars's and Earth's tropospheric polar vortices, there is a striking difference in the PV within the vortex. In Earth's stratospheric and tropospheric

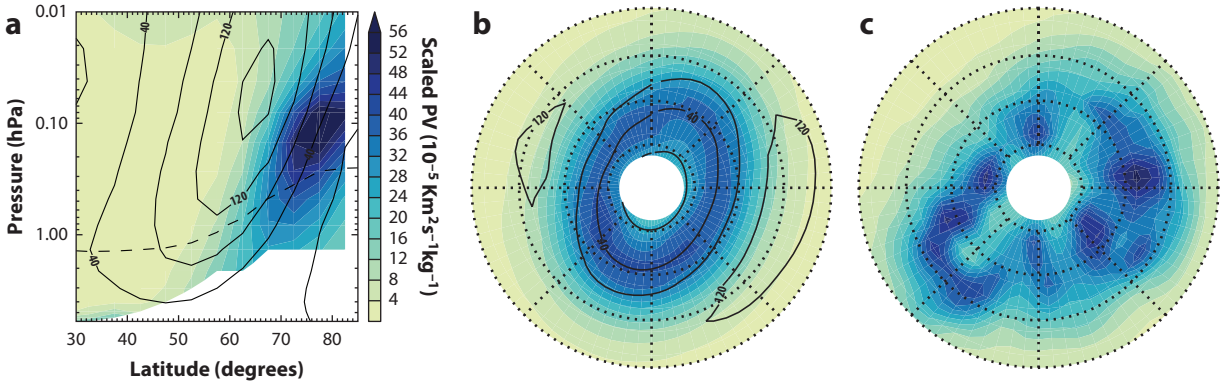

Figure 5

(*a*) Pressure–latitude plot of zonal-mean-scaled potential vorticity (PV) (*colors*; 10^{-5} K m^2 s^{-1} kg^{-1}) and zonal wind u (*solid lines*; m/s) on Mars. (*b*,*c*) Maps of (*b*) 30-sol mean and (*c*) instantaneous PV on the 300-K isentropic surface (*dashed curve* in panel *a*). All data are from the Mars Analysis Correction Data Assimilation reanalysis for Mars year 24, at northern winter solstice (solar longitude L_s = 270°). PV is scaled as PV(θ/200)$^{-5}$, where θ is the potential temperature.

Annular vortex: a vortex with an annulus of high PV surrounding a local minimum over the pole

polar vortices, the largest PV occurs at the center of the vortex (near the pole; i.e., they have a monotonic PV structure). However, observations (Banfield et al. 2004), free-running general circulation model (GCM) simulations (Barnes & Haberle 1996, Toigo et al. 2017), and meteorological reanalyses (Mitchell et al. 2015, Waugh et al. 2016, Dowling et al. 2017) for Mars all show that the maximum PV is not at the center of the vortex. Instead, there is an annulus of high PV just poleward of the jet and a local minimum over the pole (**Figure 5**). This raises two questions. First, what is the cause of the annular vortex? Second, given that an annulus of (potential) vorticity is barotropically unstable (Section 2), why does this annulus persist?

The formation of the annular vortex on Mars is thought to be caused by condensation of CO_2 in winter polar regions (Toigo et al. 2017). CO_2 is the major gas species in Mars's atmosphere, and the temperatures inside the lower polar vortex are cold enough that CO_2 condensation occurs there. The latent heat associated with this CO_2 condensation leads to the destruction of PV inside the vortex, inducing the formation of an annular PV structure. GCM simulations that include representation of latent heat associated with CO_2 condensation produce an annular PV structure similar to that observed, but when this latent heat is deliberately disabled there is a monotonic increase in the magnitude of PV from equator to pole, as found on Earth (Toigo et al. 2017). SWM simulations also show that the addition of polar heating results in a vortex with a clear annular PV structure (Rostami et al. 2018, Scott et al. 2020). Notably, the condensation of water vapor also occurs in the cold air inside Earth's stratospheric polar vortices (leading to the formation of PSCs, which play a central role in ozone depletion); however, since water vapor is only a minor constituent, the latent heating is not enough to have a significant impact on the PV.

The persistence of the annular vortex from fall to spring is surprising because an isolated band of PV is barotropically unstable (Section 2). Using SWM simulations, Seviour et al. (2017) showed that an initial Mars-like annular vortex does indeed become unstable, forming a ring of smaller vortices that coalesce to form a monopolar vortex (**Figure 6*a***). Consistent with the linear stability

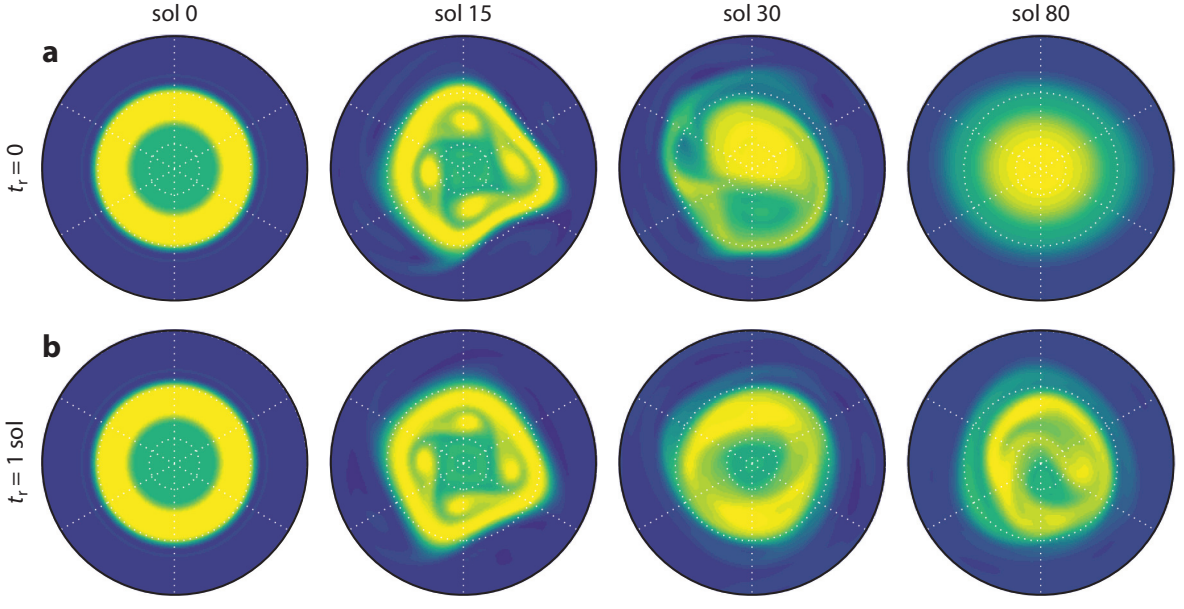

Figure 6

Maps of the evolution of potential vorticity for shallow-water model simulations of initially annular vortices with (*a*) no relaxation and (*b*) relaxation with a timescale t_r of 1 sol. Figure based on simulations described by Seviour et al. (2017).

analysis for barotropic flow on a sphere (Dritschel & Polvani 1992), Seviour et al. found that vortices with a thinner annuli or annuli with maxima nearer to the equator tended to be more unstable (have larger growth rates) than vortices that are thicker or have maxima nearer to the pole. However, by introducing a relaxation term, as shown in SWM studies of stratospheric polar vortices (e.g., Juckes 1989, Polvani et al. 1995), one can simulate a persistent annular vortex with characteristics similar to that observed in the Martian atmosphere if the relaxation timescale is similar to that of the instability (**Figure 6*b***). This suggests that the persistence of the annular vortex is due to the comparable timescale of the instability, which tends to break up the annulus, and diabatic processes (e.g., latent heating), which restore the annulus.

Maps of Martian-monthly mean PV show a near-continuous elliptical ring of high PV with roughly constant shape from fall to spring (**Figure 5*b***), which has been related to topographic-forcing (Seviour et al. 2017, Ball et al. 2021). However, the shape and orientation vary on daily timescales (e.g., **Figure 5*c***) due to transient Rossby waves propagating around the vortex edge (Scott et al. 2020, Ball et al. 2021). Unlike Earth's vortices, there do not appear to be events where large filaments of vortex air are stirred into mid-latitudes, except near the surface where both PV and ozone show filaments (Holmes et al. 2017). At these low levels there is less coherence in the polar PV, and the flow is analogous to the subvortex region in Earth's lowermost stratosphere.

The instantaneous PV from Martian reanalysis suggests that at a given instant in time there may be a series of patches of high PV rather than a continuous ring of PV (Waugh et al. 2016) (e.g., **Figure 5*c***). There is some indication of this patchy PV in the SWM simulations of Seviour et al. (2017) (**Figure 6*b***), suggesting that the patches could be due to the barotropic instability. They are also found in the SWM simulations of Rostami et al. (2018), who suggested that the patches were related to spatial variations in the latent heating. However, it is possible that these patches are an artifact of the data assimilation process. It is worth noting that early stratospheric reanalyses show PV blobs (e.g., McIntyre & Palmer 1983) that are not found in more recent reanalyses of the same period. Whether the vortex is always a continuous annulus or sometimes a ring of patches of PV is an open question.

Although the Martian vortex shape does change on a daily basis, the variation is much less than that of Earth's stratospheric vortex (Mitchell et al. 2015). There is also less interannual variation, with variations between years usually linked to changes in the atmospheric dust optical depth. Regional dust storms have been shown to cause minor disruptions to the vortices (Mitchell et al. 2015, Streeter et al. 2021), whereas global-scale dust storms that occur around the northern winter solstice cause a transient warming of the northern polar region, with a weakening of the vortex (e.g., Guzewich et al. 2016, Ball et al. 2021). This has been linked to increased dust heating rates at high southern latitudes, which drive an expansion of the descending branch of the Hadley cell into the northern polar region. GCM simulations with an obliquity greater than 35° also show a similar transient expansion of the Hadley cell and a weakening of the vortex around winter solstice, due again to increased dust heating rates at high southern latitudes (because of increased insolation) (Toigo et al. 2020). Thus, the dynamics of Martian polar vortices may have been different in past climates (as the obliquity of Mars has varied between 5° and 60° over geological timescales).

Just as on Earth, the mixing across the edge of Martian polar vortices is important for understanding the distribution of trace gases and aerosols. For example, understanding the transport of dust into polar regions is important for understanding current and past climates of Mars (as dust has a substantial impact on the radiative balance), as well as the formation of layered deposits at the Martian polar surface (which have been linked to changes in past climates). There have been very limited studies of the tracer transport within and across the polar vortices of Mars. Analyses of simulations of an idealized age tracer in a Mars GCM have shown a decrease in the age

within the polar vortex (indicating more mixing into the vortex) when it becomes annular (Waugh et al. 2019). A possible cause of this cross-jet transport could be the formation of multiple smaller-scale vortices (blobs) within the annulus (e.g., **Figure 6**), which could allow mid-latitude air leaks into the vortex core via the regions of relatively weaker PV gradients between these smaller-scale vortices. Waugh et al. (2019) also identified a near-surface subvortex region where, as in Earth's lowermost stratosphere, there is not a coherent region of high PV and more rapid exchange between the pole and mid-latitudes. More studies are required to examine transport across the vortex edge and within the subvortex region.

6. TITAN'S STRATOSPHERIC POLAR VORTICES

The polar vortices in Titan's stratosphere also share many similarities with Earth's stratospheric polar vortices (Flasar & Achterberg 2009) and, hence, with Mars's polar vortices. In particular, Titan's polar vortices occur in the winter and not summer, with low polar temperatures, steep meridional PV gradients, and peak zonal winds in mid-latitudes (Teanby et al. 2008, Achterberg et al. 2011, Sharkey et al. 2021) (**Figure 7**). In addition, similar to Earth's stratospheric vortices, there is a subsidence that leads to enhanced concentrations of hydrocarbons and nitriles produced in the mesosphere (e.g., Teanby et al. 2008, 2017; Vinatier et al. 2010), as well as the formation of polar clouds (West et al. 2016, Le Mouélic et al. 2018).

However, Titan has a broader polar vortex than Earth and Mars, with maximum winds around 40–50° in the winter hemisphere and westerlies within the tropics (where flow is called superrotation) and summer hemisphere. Titan's vortex also has an annular PV structure with a weak local minimum at the pole (e.g., Achterberg et al. 2008, Sharkey et al. 2021) and very limited zonal variations in temperature and constituent fields (Sharkey et al. 2020) (**Figure 7**). Furthermore, GCM simulations suggest a mid-winter minimum in the strength of Titan's polar vortex (Shultis et al. 2022).

The annular nature of Titan's polar vortices is also observed on Mars, as discussed in the previous section. However, the cause of the annular PV structure is likely different, as the species that condense inside Titan's polar vortices are, as on Earth, only minor species, and the magnitude of this latent heating is small and unlikely to have a significant impact on the PV. Furthermore, GCM

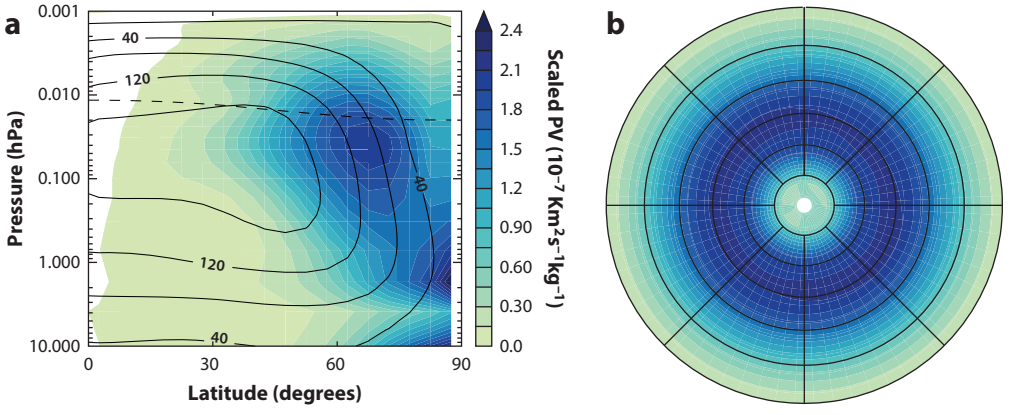

Figure 7

(*a*) Pressure–latitude plot of zonal-mean-scaled potential vorticity (PV) (*colors*; 10^{-7} K m^2 s^{-1} kg^{-1}) and zonal wind u (*solid lines*; m/s) on Saturn's moon Titan. (*b*) Map of PV (for the isentropic surface shown by the *dashed curve* in panel *a*), for northern winter solstice ($L_s = 270°$). The PV is scaled as PV$(\theta/100)^{-7/2}$, where θ is the potential temperature. Figure based on TitanWRF simulations described by Shultis et al. (2022).

simulations that do not include a representation of latent heating from polar cloud formation still produce annular vortices (Shultis et al. 2022). Thus, latent heating is not a requirement for the formation of an annulus.

The more likely cause of the annular vortex on Titan is the reduction in polar PV from a strong descent (and adiabatic warming). A similar process could also be occurring in Earth's mesosphere, where the monotonic PV structure breaks down (Harvey et al. 2009). Harvey et al. proposed that the downward motion of warm air results in a reduction of static stability ($-g\partial\theta/\partial p$), accompanying a reduction of polar PV and the creation of an annulus of PV in Earth's mesosphere. There is strong polar descent from the mesosphere into the stratosphere during winter on Titan, when the meridional circulation consists of a single cell with ascent at the summer pole and descent at the winter pole. However, an analysis of a Titan GCM simulation indicates that there is also a decrease in polar relative vorticity (from the reduced meridional temperature gradients and zonal winds accompanying the polar descent), and reductions in both static stability and relative vorticity likely contribute to the decrease in polar PV (Shultis et al. 2022).

The strong winter polar descent on Titan is connected to another difference with Earth's stratospheric polar vortices. In contrast to Earth, simulations of Titan show a mid-winter polar warming and a weakening of the vortex (and formation of an annular vortex) when there is expansion of the meridional circulation to the winter polar vortex with accompanying polar descent (Shultis et al. 2022). (The Cassini mission only made observations of Titan from the late northern winter to southern winter solstice, so there are no observations covering the complete Titan polar vortex lifecycle.) A similar expansion of the meridional circulation in mid-winter, with a polar warming, weakening of the meridional temperature gradient, and a weaker vortex, is also found in idealized GCM simulations of Titan with slow rotation rates (Guendelman et al. 2022). Furthermore, as discussed in the previous section, an expansion of the downwelling of the Hadley cell, and a polar warming and weakening of the polar vortex, also occurs on Mars in years with global dust storms (and in simulations of past climates with high obliquity).

Zonally varying disturbances are ubiquitous on the edges of Earth's and Mars's polar vortices and linked to Rossby wave propagation and wave-breaking. There is, however, a striking lack of waves on the edge of Titan's polar vortices, in both observations (Sharkey et al. 2020) and simulations (Shultis et al. 2022) (**Figure 7**). This lack of zonal variation is found throughout the Titan year, including during the winter weakening and the summer decay of the polar vortex. On Earth, the Rossby waves propagating on the vortex edge are generated in the troposphere and propagate into the stratosphere. This does not appear to be happening on Titan. Titan has a relatively flat topography and no land–sea contrast, so there may be only weak Rossby waves in the troposphere. Additionally, the Rossby radius of deformation on Titan is much ($\sim$10 times) larger than Titan's radius (unlike Earth or Mars, where the ratio is much less than 1), which results in very different Rossby wave dynamics. Furthermore, Sharkey et al. (2020) showed using linear theory (e.g., Charney & Drazin 1961) that the maximum velocity for upward propagation is much less than the measured stratospheric wind speeds on Titan (i.e., the stratospheric winds are too fast for Rossby waves to propagate into the stratosphere).

As for Earth's stratospheric and Mars's polar vortices, the transport within and across the vortex is important on Titan. Observations show dramatic differences in composition between inside and outside Titan's polar vortices, with polar concentrations of trace gas species (hydrocarbons and nitriles) formed in the mesosphere enriched by up to three orders of magnitude compared with those at low latitudes (e.g., Teanby et al. 2008, 2017; Vinatier et al. 2010). These polar enrichments, and differences between gases with differing lifetimes, have been used to infer strong polar subsidence

within the vortex and weak transport into mid-latitudes (Teanby et al. 2008, Sharkey et al. 2021). However, this transport has not been examined in detail.

7. OTHER PLANETS

As mentioned in Section 1, and reviewed by Mitchell et al. (2021), there are polar vortices on most other planets in the solar system. While similarities exist with the polar vortices on Earth, Mars, and Titan, there are also many differences. Venus also has two different features referred to as a polar vortex: A coherent planetary-scale wind pattern in mid-latitudes and a smaller, tropical cyclone-like structure at the pole (e.g., Piccioni et al. 2007, Luz et al. 2011, Garate-Lopez et al. 2013). The Venus polar vortices do not have a strong seasonality (consistent with small obliquity); the morphology and centers of the vortices are highly variable, with shape sometimes showing a dipole or S-shaped structure; and the vortices wander erratically around the pole. Saturn has, like Earth, a seasonally varying stratospheric polar vortex and a tropospheric polar vortex that exist all year round (e.g., Dyudina et al. 2008, Fletcher et al. 2018). However, Saturn's stratospheric vortex is strongest in summer and absent in winter, and the tropospheric vortex has a warm pole with similarities to Earth's tropical cyclones. Jupiter is different from all the planets, as it does not have a single coherent polar vortex on each pole, but rather clusters of vortices at both poles (Adriani et al. 2018) that have remained largely stable over three years of observation (Tabataba-Vakili et al. 2020). There remain many unanswered questions regarding the formation mechanisms and dynamics of the vortices on these planets.

The characteristics of polar vortices are likely even wider for the large, and ever growing, number of exoplanets, which include planets with characteristics not found in the solar system (e.g., tidally locked planets) (Pierrehumbert & Hammond 2019). This is likely the case even if attention is restricted to non–tidally locked terrestrial planets. Guendelman et al. (2021, 2022) recently examined the polar vortices in a suite of idealized aquaplanet GCM simulations that covered a wide range of planetary and orbital parameters. They found several distinct regimes, some of which that have similarities to the observed polar vortices, but others that have no counterpart in the solar system. The latitude and strength of the jets at the edges of the vortices were found to vary with planetary parameters, with stronger jets for moderate values of rotation rate or obliquity compared to either small or large values (**Figure 8**). Furthermore, for slow rotation rates and high obliquities, the strongest jet actually occurs in the summer rather than in the winter (Guendelman et al.

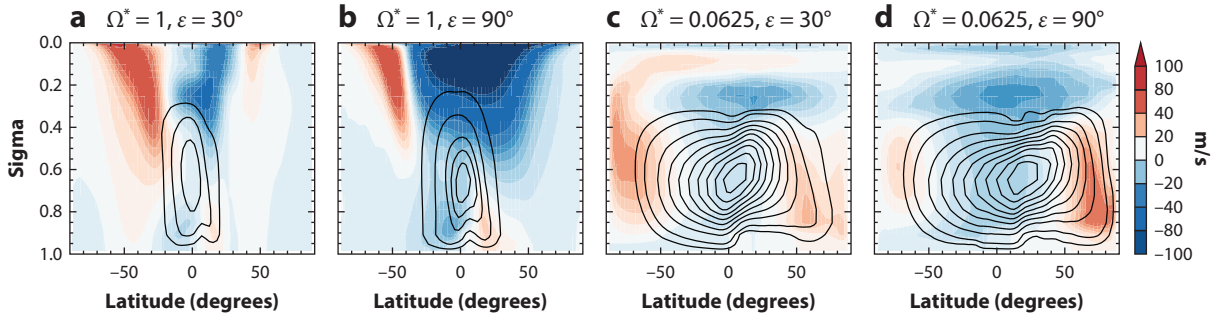

Figure 8

Zonal-mean zonal winds (*shading*) and mean meridional circulation (*contours*) at southern winter solstice, for an idealized generalized circulation model simulation by Guendelman et al. (2021), with $\Omega^* = \Omega/\Omega_{\text{Earth}}$ the rotation rate and ε the obliquity. Figure based on simulations described by Guendelman et al. (2021).

2021) (**Figure 8**). This is not observed on terrestrial bodies in the solar system and illustrates that very different polar vortices may exist on exoplanets.

SUMMARY POINTS

1. The polar vortices of Earth's stratosphere have many similarities with those on Mars and Titan: They all occur in the winter and not summer and are characterized by a coherent region of high potential vorticity (PV) in polar regions, steep meridional PV gradients and peak zonal winds at the vortex edge, and very low polar temperatures.
2. It is possible to define a planetary-scale tropospheric vortex on Earth. The edge of this vortex is equivalent to the mid-latitude dynamical tropopause and the location of upper tropospheric jets. Whether the concept of the tropospheric polar vortex adds new insights into tropospheric or stratosphere–troposphere dynamics is unclear.
3. The PV structure of the polar vortices varies among planets. On Earth there is a monopolar vortex, whereas on Mars and Titan there are annular vortices with a ring of high PV. The cause of the annulus differs between Mars (condensation of CO_2) and Titan (strong polar descent).
4. The disruption of polar vortices by Rossby waves varies among the planets, leading to large differences in the temporal and zonal variability of the vortices. At one extreme, large-amplitude Rossby waves can cause rapid disruptions of Earth's stratospheric vortex, in which the vortex is displaced off the pole or split in two. At the other extreme, Titan's polar vortices appear to be zonally symmetric with limited daily variability.
5. The seasonality of the polar vortices differs between planets. Earth's polar vortices are strongest in mid-winter, but there is mid-winter weakening of the polar vortices on Titan and, when global dust storms occur, on Mars. This weakening is due to the mean meridional circulation extending from the summer to the winter poles.
6. Transport of air across the polar vortex edge has an important influence on the distribution of radiatively important gases and particles on all three planets. This transport is generally from the outer edge of Earth's stratospheric vortex into the mid-latitudes, with limited inward transport. The transport into and out of the polar vortices on Mars and Titan is not well quantified.
7. There is likely a much wider range of polar vortex characteristics for terrestrial exoplanets than is observed for terrestrial planets in the solar system. For example, there may be terrestrial exoplanets with a summer polar vortex.

DISCLOSURE STATEMENT

The author is not aware of any biases that might be perceived as affecting the objectivity of this review.

ACKNOWLEDGMENTS

The author acknowledges the support of NASA grant 80NSSC20K0138 and NSF (National Science Foundation) grant AGS-131876. The author thanks Will Seviour and Anthony Toigo for helpful comments on the manuscript, as well as David Dritschel, Scott Guzewich, Michael

McIntyre, Alan Plumb, Lorenzo Polvani, Will Seviour, Richard Scott, Nick Teanby, and Anthony Toigo for recent and past conversations on polar vortices.

LITERATURE CITED

Abalos M, Legras B, Shuckburgh E. 2016. Interannual variability in effective diffusivity in the upper troposphere/lower stratosphere from reanalysis data. *Q. J. R. Meteorol. Soc.* 142:1847–61

Achterberg RK, Conrath BJ, Gierasch PJ, Flasar FM, Nixon CA. 2008. Titan's middle-atmospheric temperatures and dynamics observed by the Cassini Composite Infrared Spectrometer. *Icarus* 194:263–77

Achterberg RK, Gierasch PJ, Conrath BJ, Flasar FM, Nixon CA. 2011. Temporal variations of Titan's middle-atmospheric temperatures from 2004 to 2009 observed by Cassini/CIRS. *Icarus* 211:686–98

Adriani A, Mura A, Orton G, Hansen C, Altieri FR, et al. 2018. Clusters of cyclones encircling Jupiter's poles. *Nature* 555:216–19

Allen DR, Nakamura N. 2001. A seasonal climatology of effective diffusivity in the stratosphere. *J. Geophys. Res.* 106:7917–35

Andrews DG, Holton JR, Leovy CB. 1987. *Middle Atmosphere Dynamics.* San Diego, CA: Academic

Appenzeller CH, Davies HC, Norton WA. 1996. Fragmentation of stratospheric intrusions. *J. Geophys. Res.* 101:1435–56

Ayarzagüena B, Charlton-Perez AJ, Butler AH, Hitchcock P, Simpson IR, et al. 2020. Uncertainty in the response of sudden stratospheric warmings and stratosphere-troposphere coupling to quadrupled CO_2 concentrations in CMIP6 models. *J. Geophys. Res. Atmos.* 125:e2019JD032345

Baldwin MP, Ayarzagüena B, Birner T, Butchart N, Butler AH, et al. 2021. Sudden stratospheric warmings. *Rev. Geophys.* 59:e2020RG000708

Baldwin MP, Dunkerton TJ. 2001. Stratospheric harbingers of anomalous weather regimes. *Science* 294:581–84

Ball ER, Mitchell DM, Seviour WJ, Thomson SI, Vallis GK. 2021. The roles of latent heating and dust in the structure and variability of the northern Martian polar vortex. *Planet. Sci. J.* 2:203–19

Banerjee A, Fyfe JC, Polvani LM, Waugh DW, Chang KL. 2020. A pause in Southern Hemisphere circulation trends due to the Montreal Protocol. *Nature* 579:544–48

Banfield D, Conrath B, Gierasch P, Wilson JR, Smith M. 2004. Traveling waves in the Martian atmosphere from MGS TES nadir data. *Icarus* 170:365–403

Barnes JR, Haberle RM. 1996. The Martian zonal-mean circulation: angular momentum and potential vorticity structure in GCM simulations. *J. Atmos. Sci.* 53:3143–56

Boffetta G, Ecke RE. 2012. Two-dimensional turbulence. *Annu. Rev. Fluid Mech.* 44:427–51

Bracco A, McWilliams JC, Murante G, Provenzale A Weiss AJ. 2000. Revisiting freely decaying two-dimensional turbulence at millennial resolution. *Phys. Fluids* 12:2931–41

Butler AH, Seidel DJ, Hardiman SC, Butchart N, Birner T, Match A. 2015. Defining sudden stratospheric warmings. *Bull. Am. Meteorol. Soc.* 96:1913–28

Butler AH, Sjoberg JP, Seidel DJ, Rosenlof KH. 2017. A sudden stratospheric warming compendium. *Earth Syst. Sci. Data* 9:63–76

Cavallo S, Hakim GJ. 2009. Potential vorticity diagnosis of a tropopause polar cyclone. *Mon. Weather Rev.* 137:1358–71

Charlton AJ, Polvani LM. 2007. A new look at stratospheric sudden warmings. Part I: climatology and modeling benchmarks. *J. Clim.* 20:449–69

Charney J, Drazin GPG. 1961. Propagation of planetary-scale disturbances from the lower into the upper atmosphere. *J. Geophys. Res.* 66:83–109

Christiansen B. 2001. Downward propagation of zonal mean zonal wind anomalies from the stratosphere to the troposphere: model and reanalysis. *J. Geophys. Res.* 106:27307–22

Domeisen DI, Butler AH. 2020. Stratospheric drivers of extreme events at the Earth's surface. *Commun. Earth Environ.* 1:59

Dowling TE, Bradley ME, Du J, Lewis SR, Read PL. 2017. Ertel potential vorticity versus Bernoulli streamfunction on Mars. *Q. J. R. Meteorol. Soc.* 143:37–52

Dritschel DG. 1986. The nonlinear evolution of rotating configurations of uniform vorticity. *J. Fluid Mech.* 172:157–82

Dritschel DG. 1988. The repeated filamentation of two-dimensional vorticity interfaces. *J. Fluid Mech.* 194:511–47
Dritschel DG. 1989. On the stabilization of a two-dimensional vortex strip by adverse shear. *J. Fluid Mech.* 206:193–221
Dritschel DG. 1990. The stability of elliptical vortices in an external straining flow. *J. Fluid Mech.* 210:223–61
Dritschel DG. 1995. A general theory for two-dimensional vortex interactions. *J. Fluid Mech.* 293:269–303
Dritschel DG, Haynes PH, Juckes MN, Shepherd TG. 1991. The stability of a two-dimensional vorticity filament under uniform strain. *J. Fluid Mech.* 230:647–65
Dritschel DG, Polvani LM. 1992. The roll-up of vorticity strips on the surface of a sphere. *J. Fluid Mech.* 234:47–62
Dritschel DG, Saravanan R. 1994. Three-dimensional quasi-geostrophic contour dynamics, with an application to stratospheric dynamics. *Q. J. R. Meteorol. Soc.* 120:1267–98
Dyudina UA, Ingersoll AP, Ewald SP, Vasavada AR, West RA, et al. 2008. Dynamics of Saturn's south polar vortex. *Science* 319:1801
Esler JG, Polvani LM, Scott RK. 2006. The Antarctic stratospheric sudden warming of 2002: a self-tuned resonance? *Geophys. Res. Lett.* 33:L12804
Esler JG, Scott RK. 2005. Excitation of transient Rossby waves on the stratospheric polar vortex and the barotropic sudden warming. *J. Atmos. Sci.* 62:3661–82
Flasar FM, Achterberg RK. 2009. The structure and dynamics of Titan's middle atmosphere. *Philos. Trans. R. Soc. London A* 367:649–64
Fletcher LN, Orton GS, Sinclair JA, Guerlet S, Read PL, et al. 2018. A hexagon in Saturn's northern stratosphere surrounding the emerging summertime polar vortex. *Nat. Commun.* 9:3564
Garate-Lopez I, Hueso R, Sánchez-Lavega A, Peralta J, Piccioni G, et al. 2013. A chaotic long-lived vortex at the southern pole of Venus. *Nat. Geosci.* 6:254–57
Garfinkel CI, Waugh DW, Gerber EP. 2013. The effect of tropospheric jet latitude on coupling between the stratospheric polar vortex and the troposphere. *J. Climate* 26:2077–95
Garfinkel CI, Waugh DW, Polvani LM. 2015. Recent Hadley cell expansion: the role of internal atmospheric variability in reconciling modeled and observed trends. *Geophys. Res. Lett.* 42:810–24
Guendelman I, Waugh DW, Kaspi Y. 2021. The emergence of a summer hemisphere jet in planetary atmospheres. *J. Atmos. Sci.* 78:3337–48
Guendelman I, Waugh DW, Kaspi Y. 2022. Dynamics of polar vortices on terrestrial planets with a seasonal cycle. *Planet. Sci. J.* 3:94
Gutenberg B. 1949. New data on the lower stratosphere. *Bull Amer. Meterol. Soc.* 30:62–64
Guzewich SD, Toigo AD, Waugh DW. 2016. The effect of dust on the Martian polar vortices. *Icarus* 278:100–18
Harvey VL, Randall CE, Hitchman MH. 2009. Breakdown of potential vorticity–based equivalent latitude as a vortex-centered coordinate in the polar winter mesosphere. *J. Geophys. Res.* 114:D22105
Haynes PH. 1990. High-resolution three-dimensional modelling of stratospheric flows: quasi-2D turbulence dominated by a single vortex. In *Topological Fluid Mechanics*, ed. HK Moffatt, A Tsinober, pp. 345–54. Cambridge, UK: Cambridge Univ. Press
Haynes PH, Shuckburgh E. 2000. Effective diffusivity as a diagnostic of atmospheric transport: 1. Stratosphere. *J. Geophys. Res.* 105:22777–94
Hersbach H, Bell B, Berrisford P, Biavati G, Horányi A, et al. 2019. *ERA5 monthly averaged data on pressure levels from 1959 to present*. Clim. Data Store, Copernic. Clim. Change Serv., accessed May 2022. **https://doi.org/10.24381/cds.6860a573**
Holmes JA, Lewis SR, Patel MR. 2017. On the link between Martian total ozone and potential vorticity. *Icarus* 282:104–17
Holton JR, Haynes PH, McIntyre ME, Douglass AR, Rood RB, Pfister L. 1995. Stratosphere–troposphere exchange. *Rev. Geophys.* 33:403–39
Holton JR, Mass C. 1976. Stratospheric vacillation cycles. *J. Atmos. Sci.* 33:2218–25
Hoskins BJ, McIntyre ME, Robertson AW. 1985. On the use and significance of isentropic potential vorticity maps. *Q. J. R. Meteor. Soc.* 111:877–946

Jucker MN, Reichler T, Waugh DW. 2021. How frequent are Antarctic sudden stratospheric warmings in present and future climate? *Geophys. Res. Lett.* 48:e2021GL093215
Juckes MN. 1989. A shallow water model of the winter stratosphere. *J. Atmos. Sci.* 46:2934–54
Juckes MN, McIntyre ME. 1987. A high-resolution one-layer model of breaking planetary waves in the stratosphere. *Nature* 328:590–96
Kida S. 1981. Motion of an elliptic vortex in a uniform shear flow. *J. Phys. Soc. Jpn.* 50:3517–20
Kirchhoff G. 1876. *Vorlesungen über mathematische Physik*, Vol. 1: *Mechanik*. Leipzig, Ger.: Teubner-Verlag
Kolstad EW, Breiteig T, Scaife AA. 2010. The association between stratospheric weak polar vortex events and cold air outbreaks in the Northern Hemisphere. *Q. J. R. Meteorol. Soc.* 136:886–93
Kretschmer M, Coumou D, Agel L, Barlow M, Tziperman E, Cohen J. 2018. More-persistent weak stratospheric polar vortex States linked to cold extremes. *Bull. Amer. Meteorol. Soc.* 99:49–60
Lamb H. 1945. *Hydrodynamics*. New York: Dover
Lawrence ZD, Manney GL, Wargan K. 2018. Reanalysis intercomparisons of stratospheric polar processing diagnostics. *Atmos. Chem. Phys.* 118:13547–79
Le Mouélic S, Rodriguez S, Robidel R, Rousseau B, Seignovert B, et al. 2018. Mapping polar atmospheric features on Titan with VIMS: from the dissipation of the northern cloud to the onset of a southern polar vortex. *Icarus* 311:371–83
Legras B, Dritschel DG, Caillol P. 2001. The erosion of a distributed two-dimensional vortex in a background straining flow. *J. Fluid Mech.* 44:369–98
Lim EP, Hendon HH, Butler AH, Thompson DW, Lawrence ZD, Scaife AA, et al. 2021. The 2019 Southern Hemisphere stratospheric polar vortex weakening and its impacts. *Bull. Amer. Meteorol. Soc.* 102:E1150–71
Luz D, Berry DL, Piccioni G, Drossart P, Politi R, et al. 2011. Venus's southern polar vortex reveals precessing circulation. *Science* 332:577–80
Love AEH. 1893. On the stability of certain vortex motions. *Proc. London Math. Soc.* 25:18–42
Manney GL, Butler AH, Lawrence ZD, Wargan K, Santee ML. 2022. What's in a name? On the use and significance of the term "polar vortex." *Geophys. Res. Lett.* 49(10):e2021GL097617
Matsuno T. 1970. Vertical propagation of stationary planetary waves in the winter Northern Hemisphere. *J. Atmos. Sci.* 27:871–83
Matsuno T. 1971. A dynamical model of the stratospheric sudden warming. *J. Atmos. Sci.* 28:1479–94
Matthewman NJ, Esler JG. 2011. Stratospheric sudden warmings as self-tuning resonances. Part I: vortex splitting events. *J. Atmos. Sci.* 68:2481–504
McIntyre ME. 1982. How well do we understand the dynamics of stratospheric warmings? *J. Meteorol. Soc. Jpn.* 60:37–65
McIntyre ME. 1995. The stratospheric polar vortex and sub-vortex: fluid dynamics and midlatitude ozone loss. *Philos. Trans. R. Soc. Lond. A* 352:227–40
McIntyre ME, Palmer TN. 1983. Breaking planetary waves in the stratosphere. *Nature* 305:593–600
McIntyre ME, Palmer TN. 1984. The 'surf zone' in the stratosphere. *J. Atmos. Terr. Phys.* 46:825–49
Mitchell DM, Montabone L, Thomson S, Read PL. 2015. Polar vortices on Earth and Mars: a comparative study of the climatology and variability from reanalyses. *Q. J. R. Meteorol. Soc.* 141:550–62
Mitchell DM, Scott RK, Seviour WJM, Thomson SI, Waugh DW, et al. 2021. Polar vortices in planetary atmospheres. *Rev. Geophy.* 59:e2020RG000723
Moore DW, Saffman PG. 1971. Structure of a line vortex in an imposed strain. In *Aircraft Turbulence Wakes*, ed. JH Olsen, A Goldburg, M Rogers, pp. 339–54. New York: Plenum
Newman PA, Nash ER, Rosenfield J. 2001. What controls the temperature of the Arctic stratosphere during the spring? *J. Geophys. Res.* 106:19999–20010
Norton WA. 1994. Breaking Rossby waves in a model stratosphere diagnosed by a vortex-following coordinate system and a contour advection technique. *J. Atmos. Sci.* 51:654–73
O'Neill A, Oatley CL, Charlton-Perez AJ, Mitchell DM, Jung T. 2017. Vortex splitting on a planetary scale in the stratosphere by cyclogenesis on a subplanetary scale in the troposphere. *Q. J. R. Meteorol. Soc.* 143:691–705
O'Neill A, Pope VD. 1988. Simulations of linear and nonlinear disturbances in the stratosphere. *Q. J. R. Meteorol. Soc.* 114:1063–110

Piccioni G, Drossart P, Sanchez-Lavega A, Hueso R, Taylor FW, et al. 2007. South-polar features on Venus similar to those near the north pole. *Nature* 450:637–40
Pierrehumbert RT, Hammond M. 2019. Atmospheric circulation of tide-locked exoplanets. *Annu. Rev. Fluid Mech.* 51:275–303
Płotka H, Dritschel DG. 2012. Quasi-geostrophic shallow-water vortex-patch equilibria and their stability. *Geophys. Astrophys. Fluid Dyn.* 106:574–95
Plumb RA. 1981. Instability of the distorted polar night vortex: a theory of stratospheric warmings. *J. Atmos. Sci.* 38:2514–31
Plumb RA, Waugh DW, Atkinson RJ, Newman PA, Lait LR, et al. 1994. Intrusions into the lower stratospheric Arctic vortex during the winter of 1991–1992. *J. Geophys. Res.* 99:1089–105
Polvani LM, Dritschel DG. 1993. Wave and vortex dynamics on the surface of a sphere. *J. Fluid Mech.* 255:35–64
Polvani LM, Plumb RA. 1992. Rossby wave breaking, filamentation and secondary vortex formation: the dynamics of a perturbed vortex. *J. Atmos. Sci.* 49:462–76
Polvani LM, Saravanan R. 2000. The three-dimensional structure of breaking Rossby waves in the polar wintertime stratosphere. *J. Atmos. Sci.* 57:3663–85
Polvani LM, Waugh DW. 2004. Upward wave activity flux as precursor to extreme stratospheric events and subsequent anomalous surface weather regimes. *J. Clim.* 17:3548–54
Polvani LM, Waugh DW, Plumb RA. 1995. On the subtropical edge of the stratospheric surf zone. *J. Atmos. Sci.* 52:1288–309
Polvani LM, Zabusky NJ, Flierl GR. 1989. Two-layer geostrophic vortex dynamics. Part 1. Upper-layer V-states and merger. *J. Fluid Mech.* 205:215–42
Rayleigh L. 1880. On the stability, or instability, of certain fluid motions. *Proc. London Math. Soc.* 11:57–72
Reinaud JN, Dritschel DG. 2019. The stability and nonlinear evolution of quasi-geostrophic toroidal vortices. *J. Fluid Mech.* 863:60–78
Richardson MI, Wilson RJ. 2002. A topographically forced asymmetry in the Martian circulation and climate. *Nature* 416:298–301
Rong PP, Waugh DW. 2004. Vacillations in a shallow-water model of the stratosphere. *J. Atmos. Sci.* 61:1174–85
Rostami M, Zeitlin V, Montabone L. 2018. On the role of spatially inhomogeneous diabatic effects upon the evolution of Mars' annular polar vortex. *Icarus* 314:376–88
Saffman PG. 1992. *Vortex Dynamics*. Cambridge, UK: Cambridge Univ. Press
Safieddine S, Bouillon M, Paracho AC, Jumelet J, Tence F, et al. 2020. Antarctic ozone enhancement during the 2019 sudden stratospheric warming event. *Geophys. Res. Lett.* 47:e2020GL087810
Sánchez-Lavega A, Lebonnois S, Imamura T, Read P, Luz D. 2017. The atmospheric dynamics of Venus. *Space Sci. Rev.* 212:1541–616
Scaife AA, Baldwin MP, Butler AH, Charlton-Perez AJ, Domeisen DI, et al. 2022. Long-range prediction and the stratosphere. *Atmos. Chem. Physics* 22:2601–23
Scherhag R. 1948. *Neue Methoden der Wetteranalyse und Wetterprognose*. Berlin: Springer-Verlag
Schoeberl MR, Hartmann DL. 1991. The dynamics of the stratospheric polar vortex and its relation to springtime ozone depletions. *Science* 251:46–52
Scott RK, Dritschel DG. 2006. Vortex–vortex interactions in the winter stratosphere. *J. Atmos. Sci.* 63:726–40
Scott RK, Haynes PH. 2000. Internal vacillations in stratospheric-only models. *J. Atmos. Sci.* 57:3233–50
Scott RK, Polvani LM. 2004. Stratospheric control of upward wave flux near the tropopause. *Geophys. Res. Lett.* 31:L02115
Scott RK, Seviour WJM, Waugh DW. 2020. Forcing of the Martian polar annulus by Hadley cell transport and latent heating. *Q. J. R. Meteorol. Soc.* 146:2174–90
Seviour WJM. 2017. Weakening and shift of the Arctic stratospheric polar vortex: internal variability or forced response? *Geophys. Res. Lett.* 47:3365–73
Seviour WJM, Gray LJ, Mitchell DM. 2016. Stratospheric polar vortex splits and displacements in the high-top CMIP5 climate models. *J. Geophys. Res. Atmos.* 121:1400–13
Seviour WJM, Waugh DW, Scott RK. 2017. The stability of Mars's annular polar vortex. *J. Atmos. Sci.* 74:1533–47

Sharkey J, Teanby NA, Sylvestre M, Mitchell DM, Seviour WJ, et al. 2020. Mapping the zonal structure of Titan's northern polar vortex. *Icarus* 337:113441

Sharkey J, Teanby NA, Sylvestre M, Mitchell DM, Seviour WJ, et al. 2021. Potential vorticity structure of Titan's polar vortices from Cassini CIRS observations. *Icarus* 354:114030

Showman AP, Cho JY, Menou K. 2010. Atmospheric circulation of exoplanets. *Exoplanets* 526:471–516

Shultis J, Waugh DW, Toigo AD, Newman CE, Teanby NA, Sharkey J. 2022. Winter weakening of Titan's stratospheric polar vortices. *Planet. Sci. J.* 3:73

Solomon S. 1999. Stratospheric ozone depletion: a review of concepts and history. *Rev. Geophys.* 37:275–316

Streeter PM, Lewis SR, Patel MR, Holmes JA, Fedorova AA, et al. 2021. Asymmetric impacts on Mars' polar vortices from an equinoctial global dust storm. *J. Geophys. Res. Planets* 126:e2020JE006774

Tabataba-Vakili F, Rogers JH, Eichstädt, Orton GS, Hansen CJ, et al. 2020. Long-term tracking of circumpolar cyclones on Jupiter from polar observations with JunoCam. *Icarus* 335:13405

Teanby NA, Bézard B, Vinatier S, Sylvestre M, Nixon CA, et al. 2017. The formation and evolution of Titan's winter polar vortex. *Nature Commun*. 8:1586

Teanby NA, de Kok R, Irwin PGJ, Osprey S, Vinatier S, et al. 2008. Titan's winter polar vortex structure revealed by chemical tracers. *J. Geophys. Res.* 113:E12003

Thompson DW, Baldwin MP, Wallace JM. 2002. Stratospheric connection to Northern Hemisphere wintertime weather: implications for prediction. *J. Clim.* 15:1421–28

Thompson DW, Solomon S, Kushner PJ, England MH, Grise KM, Karoly DJ. 2011. Signatures of the Antarctic ozone hole in Southern Hemisphere surface climate change. *Nature Geosci.* 4:741–49

Thomson W. 1869. On vortex atoms. *Proc. R. Soc. Edinburgh* 6:94–105

Toigo A, Waugh DW, Guzewich S. 2017. What causes Mars' annular polar vortices? *Geophys. Res. Lett.* 44:71–78

Toigo A, Waugh DW, Guzewich S. 2020. Atmospheric transport into polar regions on Mars in different orbital epochs. *Icarus* 347:113816

Tung KK, Lindzen RS. 1979. A theory of stationary long waves. Part I: a simple theory of blocking. *Mon. Weather Rev.* 107:714–34

Vallis GK. 2017. *Atmospheric and Oceanic Fluid Dynamics*. Cambridge, UK: Cambridge Univ. Press

Vinatier S, Bézard B, Nixon CA, Mamoutkine A, Carlson RC, et al. 2010. Analysis of Cassini/CIRS limb spectra of Titan acquired during the nominal mission: I. Hydrocarbons, nitriles and CO_2 vertical mixing ratio profiles. *Icarus* 205:559–70

Von Helmholtz H. 1858. Über Integrale der hydrodynamischen Gleichungen, welche den Wirbelbewegungen entsprechen. *J. Reine Angew. Math.* 55:25–55

Wang L, Hardiman SC, Bett PE, Comer RE, Kent C, et al. 2020. What chance of a sudden stratospheric warming in the southern hemisphere? *Env. Res. Lett.* 15:104038

Waugh DW, Dritschel DG. 1991.The stability of filamentary vorticity in two-dimensional geophysical vortex-dynamics models. *J. Fluid Mech.* 231:575–98

Waugh DW, Dritschel DG. 1999. The dependence of Rossby wave breaking on the vertical structure of the polar vortex. *J. Atmos. Sci.* 56:2359–75

Waugh DW, Plumb RA, Atkinson RJ, Schoeberl MR, Lait LR, et al. 1994. Transport out of the stratospheric Arctic vortex by Rossby wave breaking. *J. Geophys. Res.* 99:1071–88

Waugh DW, Polvani LM. 2010. Stratospheric polar vortices. In *The Stratosphere: Dynamics, Transport, and Chemistry*, ed. LM Polvani, AH Sobel, DW Waugh, pp. 43–57. Geophys. Monogr. Ser. 190. Washington, DC: Am. Geophys. Union.

Waugh DW, Randel WJ, Pawson S, Newman PA, Nash ER. 1999. Persistence of the lower stratospheric polar vortices. *J. Geophys. Res.* 104:27191–201

Waugh DW, Sobel AH, Polvani LM. 2017. What is the polar vortex and how does it influence weather? *Bull. Amer. Meteor. Soc.* 98:37–44

Waugh DW, Toigo AD, Guzewich SD. 2019. Age of Martian air: time scales for Martian atmospheric transport. *Icarus* 317:148–57

Waugh DW, Toigo AD, Guzewich SD, Greybush SJ, Wilson RJ, Montabone L. 2016. Martian polar vortices: comparison of reanalyses. *J. Geophys. Res.* 121:1770–85

West RA, Del Genio AD, Barbara JM, Toledo D, Lavvas P, et al. 2016. Cassini Imaging Science Subsystem observations of Titan's south polar cloud. *Icarus* 270:399–408

Zalucha AM, Plumb RA, Wilson RJ. 2010. An analysis of the effect of topography on the Martian Hadley cells. *J. Atmos. Sci.* 67:673–93

Zhang J, Tian W, Chipperfield MP, Xie F, Huang J. 2016. Persistent shift of the Arctic polar vortex towards the Eurasian continent in recent decades. *Nat. Climate Change* 6:1094–99